Vertical motion estimated from combined ARGO and altimetry observations

Ananda Pascual[1], S. Ruiz[1], B. Buongiorno Nardelli[2,3], S. Guinehut[4], Y. Drillet[5], S. Mulet[4], M-H. Rio[4], F. Bignami[2], G. Larnicol[4], J. Tintoré[1,6]

[1]IMEDEA(CSIC-UIB), Esporles, Spain, contact: ananda.pascual@imedea.uib-csic.es
[2] Istituto di Scienze dell'Atmosfera e del Clima, Roma, Italy
[3] presently at Istituto per l'Ambiente Marino Costiero, Napoli, Italy
[4] Collecte Localisation Satellites, Toulouse, France
[5] Mercator-Ocean, Toulouse, France
[6] Balearic Islands Coastal Observing and Forecasting System – SOCIB, Mallorca, Spain

Introduction: importance of vertical motion

Vertical motion associated with **mesoscale** and **sub-mesoscale** oceanic features is of fundamental importance for the exchanges of heat, fresh water and biogeochemical tracers between the surface and the ocean interior. Unfortunately, direct measurements of the vertical velocity are difficult to obtain for usual values (order 10's m/day). Various indirect methodologies have thus been proposed to estimate vertical velocity from observed density and geostrophic velocity fields. The most used technique is based on the solution of the quasi-geostrophic (QG) Omega equation (Tintoré et al. 1991; Buongiorno Nardelli et al. 2001; Pascual et al. 2004; Ruiz et al. 2009).

Objectives & Context

The objective of this study is to estimate and analyze vertical exchanges associated with mesoscale dynamics and of their interannual variability from an observational data set. This work is performed in the framework of MESCLA, a R&D proposal funded within MyOcean EU FP7 project. MESCLA aims at:

(1) Applying QG diagnostics to MyOcean products (model and observation based).

(2) Comparing its results with corresponding primitive equation solutions.

(3) Testing alternative techniques to combine satellite and in situ observations.

Input Data

ARMOR3D reanalysis

- 3D fields of temperature, salinity and steric height derived from an observational-based product that combines satellite (SST and altimetry) and in-situ (Argo profiling floats, XBT, CTD and moorings) data (Guinehut et al. 2001)

Method

Preprocessing

- Vertical interpolation: 10:10:1000 m
- Horizontal interpolation: regular grid (1/3º)
- Conversion of data files to be ingested into the fortran code for the estimation of vertical velocity

QG vertical velocities: Omega equation. Vector Q formulation

$$f^2 \frac{\partial^2 \omega}{\partial z^2} + \left(\frac{\partial^2}{\partial x^2} + \frac{\partial^2}{\partial y^2}\right)\left(N^2 \omega\right) = \nabla_h Q$$

$$Q = \left[2f\left(\frac{\partial V}{\partial x}\frac{\partial U}{\partial z} + \frac{\partial V}{\partial y}\frac{\partial V}{\partial z}\right), -2f\left(\frac{\partial U}{\partial x}\frac{\partial U}{\partial z} + \frac{\partial U}{\partial y}\frac{\partial V}{\partial z}\right)\right]$$

Hoskins et al (1978) $\frac{|\mathbf{u}_a|}{|\mathbf{U}|} = O(\varepsilon) \qquad \varepsilon \ll 1$

where (U,V) are the geostrophic velocity components, *N* Brunt-Vaisala frequency and *f* the Coriolis parameter.

By assuming a BC for ω and from a 3D snapshot of the density field, the vertical velocity can be inferred.

First tests:

w = 0 at the upper, lower and lateral boundaries

N is considered to vary only in the vertical: N = N(z).

Output Data

MESCLA vertical velocity re-analysis

Period: 1993-2009
Temporal resolution: monthly
Horizontal spatial resolution: 1/3° grid
Vertical levels: 10:10:1000
Domain: Gulf Stream

Auxiliary Data

Net Primary Production (NPP) data (gross photosynthetic carbon fixation minus the carbon respired to support maintenance requirements): provided by Oregon State University based on the original description of the Vertically Generalized Production Model (VGPM) (Behrenfeld & Falkowski 1997). More details at: http://www.science.oregonstate.edu/ocean.productivity).
Period: 1998 - 2002 (seawifs based)
2003 - 2010 (modis based)
Temporal resolution: monthly files (weekly also available at the server)
Spatial resolution: 1/6°

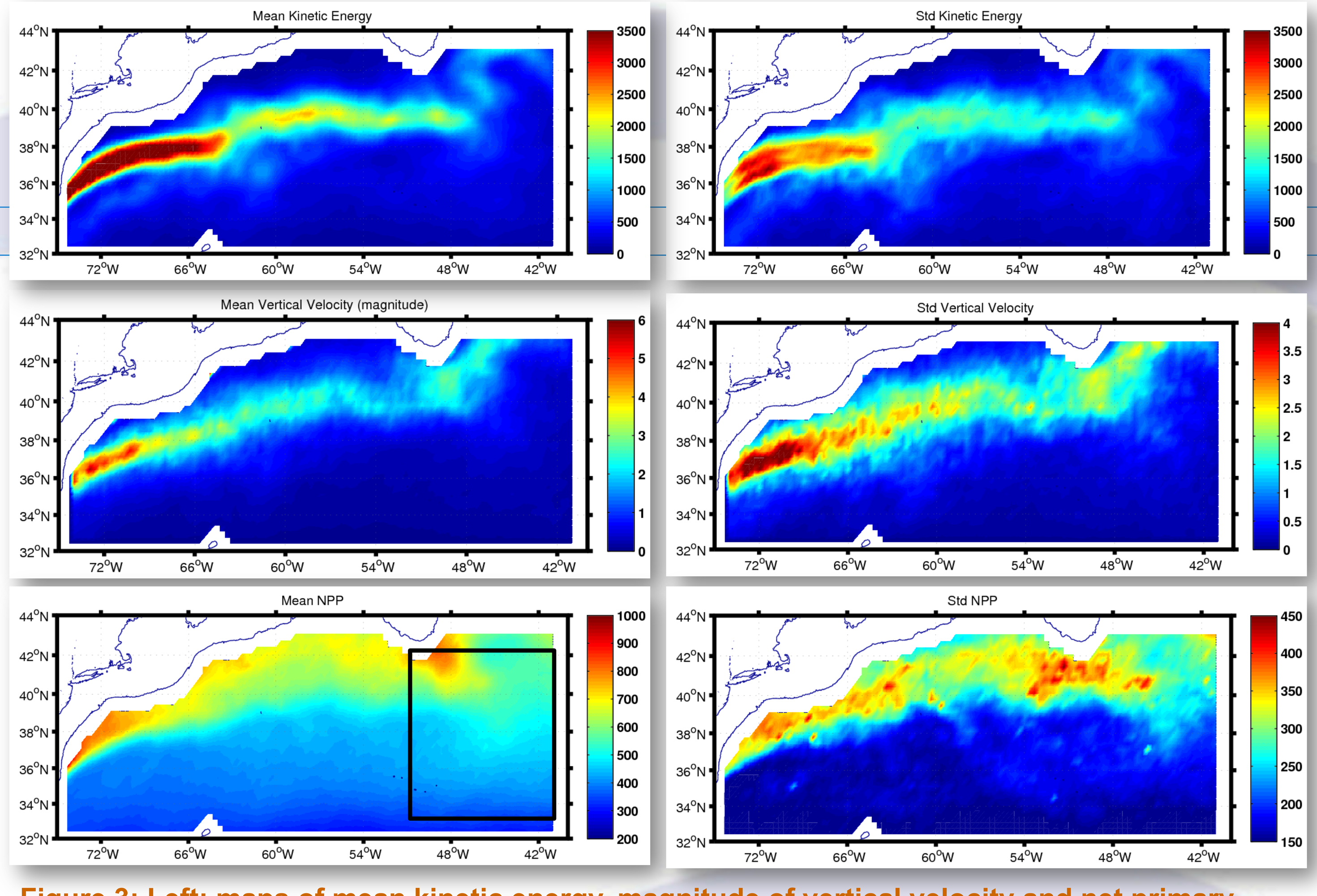

Figure 3: Left: maps of mean kinetic energy, magnitude of vertical velocity and net primary production, averaged over the common period of study (1998-2009). Right panels: as left panels but for standard deviation. Units are indicated in Figure 1. Isolines are 0 and 1000 m. Areas shallower than 1000 m (bottom boundary in the QG w computation) have been masked.

QG vertical velocity analysis in the Gulf Stream

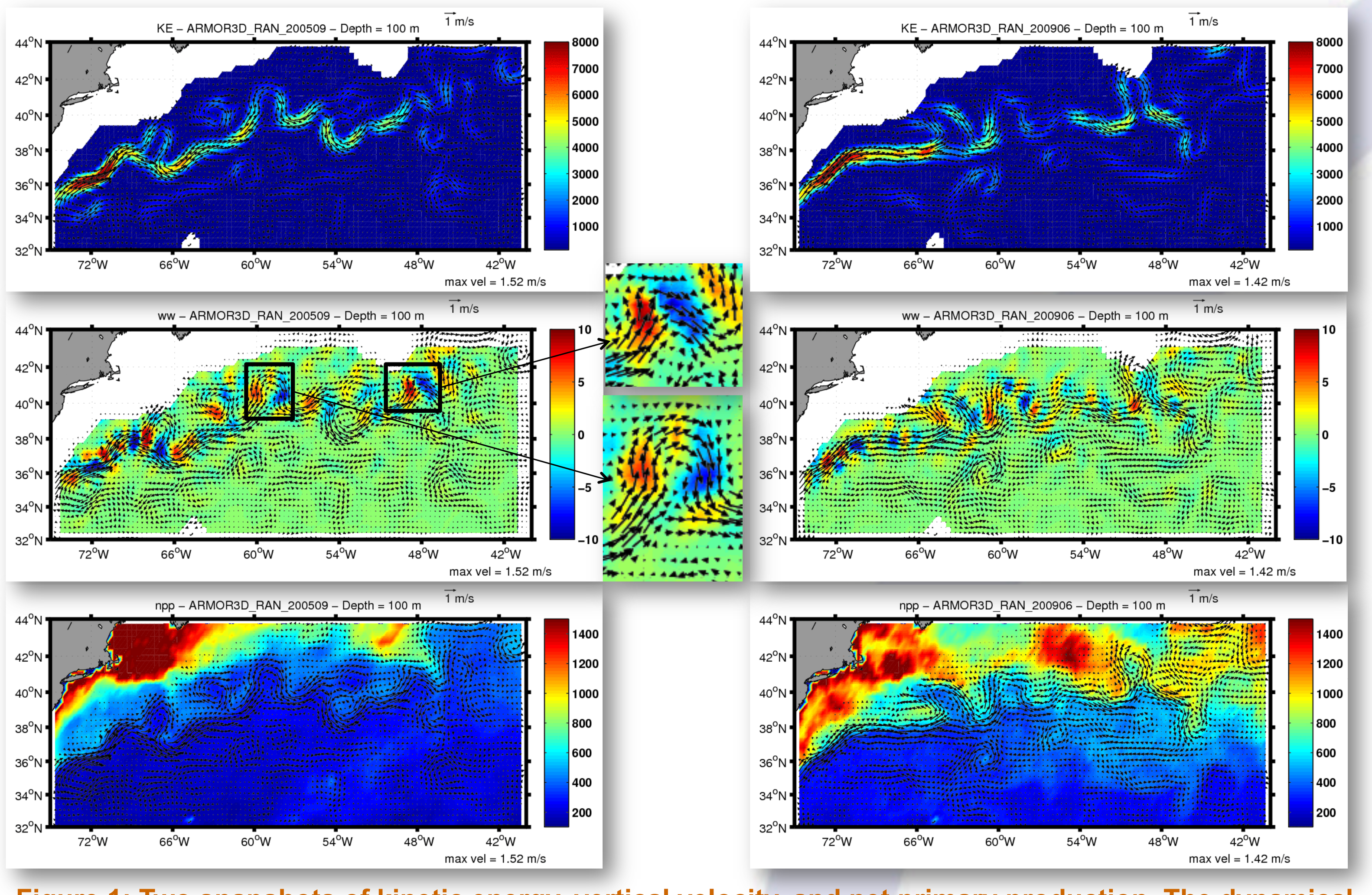

Figure 1: Two snapshots of kinetic energy, vertical velocity, and net primary production. The dynamical fields are shown at 100 m, which is considered the average photic layer in the Gulf Stream area (Oschlies and Garçon, 1998). Units are $cm^2\ s^{-2}$, $m\ day^{-1}$ and $mg\ C\ m^{-2}\ day^{-1}$, respectively.

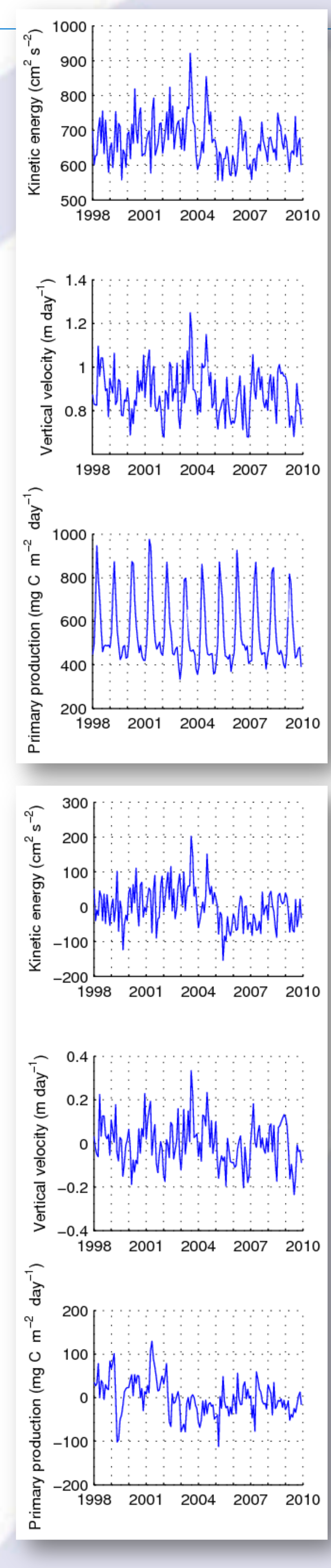

Figure 2: Top: Time series of mean kinetic energy, magnitude of vertical velocity and net primary production, averaged over the area of study. Bottom: as top panels but for deseasoned time series.

Figure 1 shows that intense vertical motion is located in areas of strong KE (along the Gulf Stream) but the relationship is not linear. Upwelling/downwelling take place upstream/downstream of meander troughs, as predicted by QG theory (Cushman-Roisin, 1994).

The horizontal geostrophic fields derived from ARMOR reveal the presence of eddies and meanders of the Gulf Stream, that match very well with the signals present in the NPP field. This good agreement, which is generalized for the whole time series analyzed, constitutes the first qualitative validation of the ARMOR fields with independent data, in terms of identification and characterization (position, size and shape) of frontal structures. NPP patterns also show a N-S gradient with an increase in coastal areas. The jet of the Gulf Stream acts as a barrier and, at the same time, as an effective mechanism of exporting organic matter from the coastal to the open ocean. Thus, at first stage, NPP can be considered as a tracer since the horizontal advection is the dominant signal. One of the objectives of this work is to assess whether the spatial and temporal variability (at the scales ranging from seasonal to interannual) depicted by NPP can be partially explained by vertical motion. The hypothesis behind these relationships relies on the fact that significant variations in the vertical exchange associated to mesoscale dynamics could impact both the ocean capacity to absorb CO2 and the nutrient availability for phytoplankton growth.

We further examine the variability of the vertical velocity through standard analysis (spatial and temporal means, empirical orthogonal function decomposition, interannual and seasonal variability). While there is an evident correlation between w and KE (especially the two peaks in 2003 and 2004), the existence of a marked seasonal cycle with weak interannual variability in the NPP signal masks any possible agreement with the other variables (Figure 2 top). When this annual cycle is removed and the residual NPP signal is compared with w time series (Figure 2 bottom), very low correlation is obtained between both variables. We speculate that this is due to the predominance of horizontal advection that masks the possible influence of vertical velocities on the modulation of NPP.
The temporal mean of NPP shows that the maximum values are located in the coastal zone, close to the Gulf Stream separation, and at 42ºN and 48ºW. This area corresponds to a permanent gyre (Rio et al., 2011) that may cause an average increase of NPP (topographic effects can be also important). In this zone (square box of Figure 3), a significant correlation is retrieved for the latitudinal and longitudinal behavior of the three variables analyzed (Figure 4).

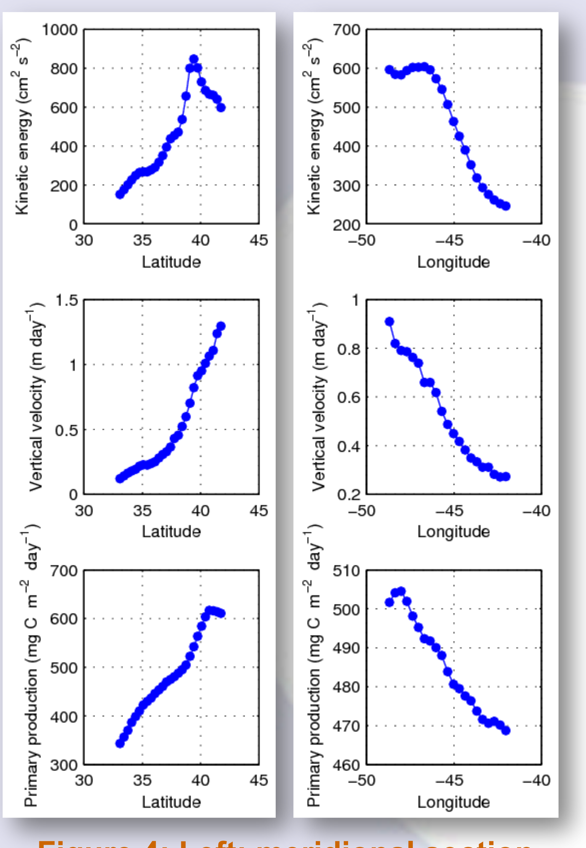

Figure 4: Left: meridional section of mean kinetic energy, vertical velocity magnitude and net primary production, averaged over the common period of study (1998-2009). Right: as left panels but for zonal section. The area averaged is shown in Figure 3.

References

Behrenfeld, MJ, PG Falkowski, Photosynthetic rates derived from satellite-based chlorophyll concentration. Limnology and Oceanography, Volume 42: 1-20, 1997.
Buongiorno Nardelli B., Sparnocchia S., Santoleri R., Small mesoscale features at a meandering upper ocean front in the western Ionian Sea, J. Phys. Ocean., Vol. 31, 8, 2227–2250, 2001.
Cushman-Roisin, B. Introduction to Geophysical Fluid Dynamics. Prentice-Hall, 1994.
Guinehut S., P.-Y. Le Traon, G. Larnicol and S. Philipps, Combining Argo and remote-sensing data to estimate the ocean three-dimensional temperature fields – a first approach based on simulated observations, J. Mar. Sys., 46, 85-98, 2004.
Hoskins, B. J., I. Draghici, and H. C. Davies, A new look at the omega-equation, Q. J. R. Meteorol. Soc., 104, 31–38, 1978.
Oschlies, A. and Garçon, V.: Eddy-induced enhancement of primary production in a model ofthe North Atlantic Ocean, Nature, 394, 266–269, 1998.
Pascual, A., D. Gomis, R. L. Haney, and S. Ruiz, A quasigeostrophic analysis of a meander in the Palamos Canyon: Vertical velocity, geopotential tendency, and a relocation technique, Journal of Physical Oceanography, 34(10), 2274-2287, 2004.
Rio, M. H., S. Guinehut, and G. Larnicol, New CNES-CLS09 global mean dynamic topography, J. Geophys. Res., 116, C07018, 2011.
Ruiz, S., A. Pascual, B. Garau, I. Pujol, and J. Tintoré, Vertical motion in the upper ocean from glider and altimetry data, Geophys. Res. Lett., 36(14), 2009.
Tintoré, J., D. Gomis, S. Alonso, and G. Parrilla, Mesoscale dynamics and vertical motion in the Alboran Sea, J. Phys. Oceanogr., 21, 811–823, 1991.

Summary & Future work

- This study is a contribution towards improving our understanding of the net effect of mesoscale variability on water mass formation and transport at global scale, as well as on its impact on the biochemical tracer redistribution and consequent marine ecosystem response.
- Further steps:
  - To investigate the potential impact of QG velocities on primary production in specific regions and events.
  - To perform sensitivity analysis of boundary conditions in the QG integration (topographic constraint).